Available online at www.sciencedirect.com

jmr&t Journal of Materials Research and Technology

www.jmrt.com.br

Original Article

Processing and characterization of amorphous magnesium based alloy for application in biomedical implants

Telma Blanco Matias, Gabriel Hitoshi Asato, Bruno Torquato Ramasco, Walter José Botta, Claudio Shyinti Kiminami, Claudemiro Bolfarini*

Materials Engineering Department, Universidade Federal de São Carlos (UFSCar), São Carlos, SP, Brazil

ARTICLE INFO

Article history:
Received 23 September 2013
Accepted 18 March 2014
Available online 14 April 2014

Keywords:
Magnesium-based alloys
Biomaterials
Bioabsorbable implants
Amorphous

ABSTRACT

Magnesium-based bulk metallic glasses are attractive due to their single-phase, chemically homogeneous alloy system and the absence of second-phase, which could impair the mechanical properties and corrosion resistance. However, one of the unsolved problems for the manufacturability and the applications of bulk metallic glasses is that their glass-forming ability is very sensitive to the preparation techniques and impurity of components since oxygen in the environment would markedly deteriorate the glass-forming ability. Therefore, the aim of this study was to establish proper processing conditions to obtain a magnesium-based amorphous ternary alloy and its characterization. The final composition was prepared using two binary master alloys by melting in an induction furnace. Carbon steel crucible was used in argon atmosphere with and without addition of SF_6 gas in order to minimize the oxygen contamination. The microstructure, amorphous nature, thermal properties and chemical analysis of samples were investigated by scanning electron microscopy (SEM), X-ray diffraction (XRD), differential scanning calorimetry (DSC) and inductively coupled plasma emission spectrometry, respectively. The oxygen content of the as-cast samples was chemically analyzed by using carrier gas hot extraction (O/N Analyzer TC-436/LECO) and was kept bellow 25 ppm (without SF_6) and 10 ppm (with SF_6). Bulk samples were produced by rapid cooling in a cooper mold until 1.5 mm thickness, with amorphous structures being observed up to 2.5 mm.

1. Introduction

Recently, a large number of materials have been studied for possible application in the human body. The initial condition for limiting such materials is that they must be compatible with the biological system, causing no toxic, allergic, inflammatory, or cancerous effects. Therefore, the number of currently used materials as biomedical implants is quite limited and includes stainless steel, alloy of cobalt–chrome,

* *Corresponding author.*
E-mail addresses: telmabmatias@gmail.com, telma_blanco@hotmail.com (T.B. Matias).
http://dx.doi.org/10.1016/j.jmrt.2014.03.007

titanium and titanium based alloys, several ceramics, polymers and composites. The use of magnesium-based alloys as biomedical implants dates from the early twentieth century and has been investigated up to now. The interest in magnesium alloys is mainly due to its excellent mechanical properties, biocompatibility, biodegradation properties and relatively low cost. Among the numerous advantages of using magnesium alloys as biomedical implants, the more attractive one is their low density, ranging from 1.74 to 2.00 g/cm^3. The low elastic modulus, from 41 to 45 GPa is also very desirable when compared to stainless steel (about 200 GPa), cobalt based alloys (about 230 GPa), and titanium (about 115 GPa). The higher the similarity between the elastic modules of the implant and bone, the smaller the problem of stress shielding, and consequently, the bone restoration process takes place more efficiently [1]. Moreover, literature reports indicate that the corrosion is accompanied by the formation of a layer of calcium phosphate on bone, which favors the osteosynthesis, and the corrosion product is a soluble oxide, which is nontoxic and is eliminated through urine [2]. It is known that pure Mg has poor mechanical properties that can be effectively improved by the addition of appropriate alloying elements [3]. However, the range of alloying elements appropriate to processing biodegradable magnesium alloys is rather limited by problems of biocompatibility. Among the possible alloying elements, Ca, Zn, Mn are worth to be mentioned and, in addition, a small amount of rare earths with low toxicity can be tolerated in the human body. Calcium is an element studied in bioabsorbable magnesium alloys due to its suitable chemical and physical properties and also for being a major component of the human body. Its low density (1.55 g/cm^3) enables the production of magnesium based binary alloys with density similar to the bone. Furthermore, it is known that magnesium is required for the incorporation of calcium into bone, leading to the belief that the release of Ca and Mg ions may be beneficial to bone consolidation. Based on these premises, Li et al. [4] developed Mg–Ca binary alloys to be used as biodegradable implants. Unfortunately, the materials showed no homogeneous corrosion properties with surface defects reported as pitting corrosion, resulting in a rapid loss of resistance of the parts. In contrast, *in vivo* cytotoxicity tests have qualified these alloys as materials for biodegradable implants. The corrosion mechanism of crystalline magnesium-based alloys in electrolytic solutions was described by Staiger et al. [1], who reported the formation of a protective oxide layer $Mg(OH)_2$. However, in environments containing chloride ions this layer is destroyed by pitting corrosion, which accelerates the degradation of the material. In addition, hydrogen is a corrosion product of magnesium, and the bubbles formed by the oxidation of the magnesium present in the implant can cause pain and discomfort to the patient, requiring its removal by means of puncturing. In the worst case, when large hydrogen bubbles are present in the blood circulation system, there will be a risk that these bubbles may block the blood stream, causing death of the patient [5]. In an attempt to minimize this effect, researchers studied the effect of adding Zn to Mg and found that concentrations above 28% provide the formation of a passivated layer rich in zinc and oxygen and reduction of the amount of H_2 released to acceptable levels [6]. This condition is possible only in glassy alloys that promote an expansion of the solubility of Zn in Mg, avoiding the formation of undesirable intermetallic phases. In view of the fact that the amorphous is a metastable state for metals, a specific process is necessary to obtain it. The three major contributing factors to glass formation are significantly different atomic radii of the elements involved, generally higher than or equal to 12%; high negative heat of mixing; and multicomponent alloy system (with more than three components) [7]. Studies revealed that the addition of a small percent of Ca upgrade the GFA in Mg–Zn alloys [8], probably because the introduction of Ca into this system qualifies the alloy to follow the three empirical rules leading to high GFA. Bulk metallic glasses can be synthesized either by solidification or by solid state processing. The rapid quenching of the melt in water is the oldest of all techniques and the high rate of cooling prevents the formation of detectable crystalline phases and glass formation could be achieved [7]. Nowadays, the modern techniques of preparing bulk metallic glasses include pouring the cast in a copper mold to obtain high cooling rates. Based on these assumptions and in previous studies of our research group, which indicated a higher glass forming ability (GFA) for ternary Mg–Zn–Ca alloys with calcium concentrations around 5% [9], we elected the composition of the ternary magnesium alloy studied in this work. The effect of addition of SF_6 gas to the argon atmosphere, which is usually used in this type of fusion, was also evaluated. The use of SF_6 gas has been indicated in the literature as protective against oxidation [4,10–13]. This procedure was adopted to minimize oxygen contamination in the fusion environment, thereby helping to reach the amorphous alloy, where oxygen contents below 250 ppm are needed [14].

2. Experimental procedure

Chemical elements of high purity (over 99.9%) were used. They were pickled in appropriate acidic solutions, washed in an ultrasonic bath in acetone, and dried with a dryer. For calcium, this step was not needed because it is commercially available in sealed flasks under argon atmosphere. Initially, two binary alloys were melted with eutectic composition of $Mg_{89.5}Ca_{10.5}$, whose melting point is 516.5 °C, and $Mg_{72}Zn_{28}$, with a melting point of 340 °C. The ingots of selected compositions were prepared in a centrifugal induction furnace (Linn High Therm, Model Titancast 700 VAC), in argon ultrapure 5.0 (99.999%) with and without addition of SF_6 3.0 (99.9%). This equipment promotes the induction heating of the metal charge placed in a cylindrical steel crucible. From the processing of binary alloys, the $Mg_{65}Zn_{30}Ca_5$ ternary alloy was obtained. To prepare the wedge-like geometry, a copper mold was used in which molten material was poured. The assembly (crucible + mold) was rotated at 400 rpm so that centrifugal force caused the liquid metal to fill the mold in a very short time. In addition, melt-spun ribbons were produced to evaluate the GFA of the particular composition. This melt spinning process is widely used for production of glassy alloys because it provides very high cooling rates of approximately 10^5–10^6 K s^{-1}. The alloys were characterized using X-ray diffraction (XRD) and differential scanning calorimetry (DSC). XRD measurements were performed on a diffractometer (Siemens, D5005 model) using Cu-Kα radiation (α = 1.5418 Å) and scanning 2°/min, from 10°

Table 1 – Quantitative chemical analysis of as-cast alloy melted in argon + SF_6 atmosphere.

Element	Theory $Mg_{65}Zn_{30}Ca_5$ % (w/w)	Experimental $Mg_{65}Zn_{30}Ca_5$ % (w/w)
Ca	5.50	5.33 ± 0.11
Mg	42.36	42.44 ± 1.32
Zn	52.53	52.88 ± 0.72
O	–	0.0010 ± 0.0001

Table 2 – Quantitative chemical analysis of as-cast alloy melted in argon atmosphere.

Element	Theory $Mg_{65}Zn_{30}Ca_5$ % (w/w)	Experimental $Mg_{65}Zn_{30}Ca_5$ % (w/w)
Ca	5.50	5.22 ± 0.16
Mg	42.36	41.09 ± 0.55
Zn	52.53	50.46 ± 0.90
O	–	0.0025 ± 0.0003

to 90°. The thermal characterization was performed by DSC (Netzsch, 404 DSC model) with a heating rate of 40 K/min, under ultrapure argon atmosphere flowing at 150 mL/min. The microstructure analyses were performed using a scanning electron microscope (FEI, INSPECT S50 model). The oxygen content of the as-cast samples was chemically analyzed by using a carrier gas hot extraction (O/N Analyser TC-436/LECO), while the levels of the alloying elements were determined by inductively coupled plasma optical emission spectrometry (ICP OES, VISTA equipment from Varian).

3. Results and discussion

The chemical compositions of the experimental binary alloys were determined and the results indicated that the final compositions were close to the target for $Mg_{89.5}Ca_{10.5}$ and $Mg_{72}Zn_{28}$ alloys. The Ca containing alloy presented an overall yield of 88.8%, probably due to Ca and Mg oxidation/evaporation, since a temperature over the melting temperature of Ca (842 °C) is necessary for complete homogenization, which is much higher than the melting temperature of Mg (650 °C). In contrast, in the case of the $Mg_{72}Zn_{28}$ alloy, the yield was considerably higher, 99.8%, as the working temperature lies slightly over the melting temperature of Mg (650 °C), which attenuates the oxidation/evaporation tendency of the alloying elements. In order to obtain a ternary alloy with an amorphous structure, stoichiometric quantities of both alloys were weighed with the necessary addition of pure Zn, and melted to obtain the final composition $Mg_{65}Zn_{30}Ca_5$. The results for the chemical analysis showed a good agreement between the calculated and the experimental values, as well as a low content of oxygen (10 ppm ± 1 ppm) owing to the use of SF_6 gas added to the argon during the fusion process. This oxygen content is considerably low and suffices for amorphous phase formation. The results showed a slight increase in the oxygen content from 10 ppm to 25 ppm without SF_6 addition, which is still well below the admissible value of 250 ppm [14]. As the addition of SF_6 is difficult to be controlled and it represents a net negligible charge to the environment, some attempts were carried out to avoid its utilization and only argon was used (99.999%) in all steps of melting. Therefore, the use of SF_6 was discontinued and argon 99.999% was used for sample preparation. The results are shown in Tables 1 and 2.

In her dissertation work, Danez [9] processed several magnesium based alloys in order to evaluate their glass-forming ability. In this study, the author establishes three different processing routes for the samples. After characterization, it was observed that only four of the twelve alloys processed presented amorphous phase. Moreover, the oxygen contents analyzed by energy dispersive spectroscopy (EDS) were much higher than the admissible value of 250 ppm [14], including for the amorphous alloys. Although all melting processes were carried out in inert argon atmosphere, the results ranged from 1.98 to 6.78% m/m. However, the EDS technique enables the achievement of semi-quantitative analyses, while the carrier gas hot extraction technique, used in the present study, permits quantitative analysis. In the carrier gas hot extraction technique, approximately 100 mg is used, which is quite representative of the original solid. Thus, it is believed that carrier gas hot extraction is the most suitable technique for the determination of oxygen content in metallic materials in general. Unfortunately, information on materials processing with less contamination and more efficiency, or even on the most appropriate technique for their characterization, is not widely discussed in the literature. Nevertheless, this information is of fundamental importance when a new material is processed, especially for alloys containing Ca and Mg because of their high reactivity. Aside of this, it is important to note that the preparation of the binary master alloys is a key factor for the success of the final melting process. Contrary to this work, Danez [9] melted all the elements in one step for obtaining the target composition, a procedure that contributed to the high level of oxygen in the resulted alloy, a consequence of the high temperature necessary for melting Ca, which lies well above the melting temperatures of Mg and Zn.

The melting points of the alloys processed were determined by DSC analyses on cast samples and the fusion ranges found for the binary alloys were 344–481 °C for $Mg_{72}Zn_{28}$ and 518–602 °C for $Mg_{89.5}Ca_{10.5}$, with endothermic peaks at 369 °C and 542 °C, respectively (Fig. 1). It is possible to observe that the work temperature was 300 °C lower than the melting temperature of Ca, thereby avoiding losses and oxidation.

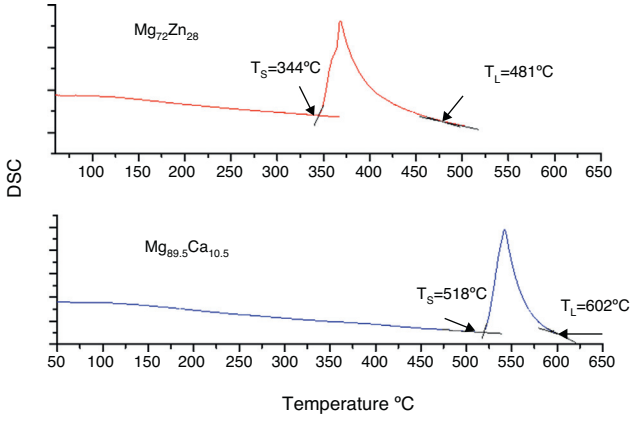

Fig. 1 – DSC thermograms of the binary alloys.

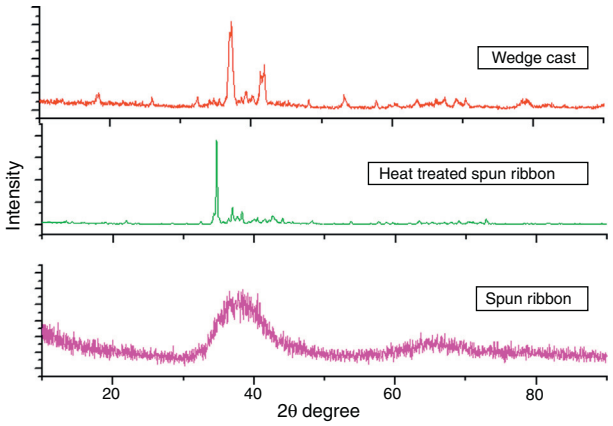

Fig. 2 – X-ray diffraction patterns of as-cast melt spun ribbon, heat-treated ribbon and thickest region of the wedge cast in copper mold.

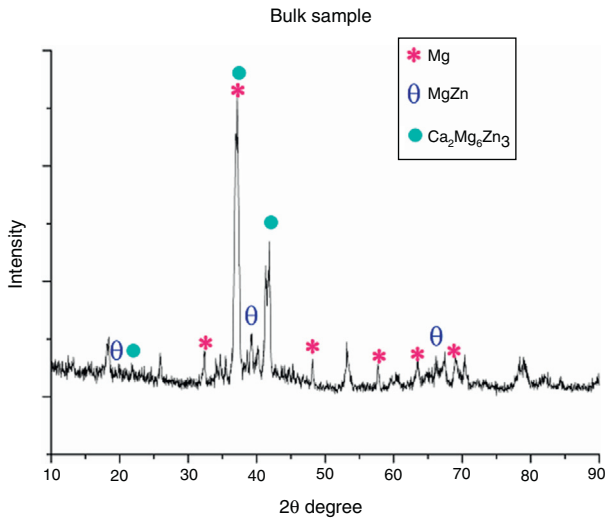

Fig. 3 – X-ray diffraction pattern corresponding to the crystalline part of the wedge cast in the copper mold.

Based on the present results, we can conclude that the procedure herein developed was efficient, allowing the achievement of the ternary Mg-based alloy with low oxygen content, regardless of the inert atmosphere used during melting. According to Xi et al. [14], oxygen adversely affects the formation of the amorphous phase, reacts with magnesium oxide forming a structure similar to the Laves phase, which favors heterogeneous nucleation, disfavoring the formation of amorphous material.

A ribbon and a wedge were processed in order to evaluate the presence of amorphous phase and its depth. The thickness and width of the melt-spun ribbon prepared for GFA evaluation were measured with micrometer accuracy of ±5 μm. The thickness ranged between 50 and 60 μm and average width was 2.6 mm. Qin et al. [15] processed the same alloy, $Mg_{65}Zn_{30}Ca_5$, simultaneously to this study, to assess its mechanical and corrosion properties. They processed the ribbons using the melting spinning technique and found amorphous ribbons with 35 μm in thickness and 3 mm in width.

Fig. 2 shows the X-ray (XRD) diffraction patterns of the melt-spun ribbon, melt-spun ribbon subjected to heat treatment at 280 °C for 30 min, and a crystalline portion of the wedge-like sample (thickest region). The diffraction patterns indicate different characteristics and the melt-spun ribbon presents a unique pattern typical of amorphous structure characterized by the presence of a single diffuse peak. The patterns for the other two samples exhibited diffraction peaks of crystalline structure with peaks of different width, which indicate differences in the grain size, probably due to the heat treatment to which the amorphous ribbon was subjected and a possible texture in the sample cast in permanent mold.

Basically, the XRD patterns of the crystalline samples show the presence of Mg (possibly with Zn and Ca in solid solution), MgZn as a primary phase, and a eutectic composition probably with the presence of MgZn + Mg + $Mg_6Zn_3Ca_2$, as illustrated in detailed in Fig. 3 for the thickest region of the wedge.

Fig. 4 shows the diffraction patterns of three different regions of the wedge cast in the copper mold with 1 mm, 1.5 mm and 2 mm thickness. It is possible to observe that the amorphous phase was obtained for 1 and 1.5 mm. On the other hand, the 2 mm thickness presented crystalline phases that relate well to the ones observed in the thickest regions of the wedge, whose diffraction pattern was presented in Fig. 3.

Cao et al. [16] also processed the alloy $Mg_{65}Zn_{30}Ca_5$ to evaluate its *in vitro* degradation rate and cell viability. The results obtained by these authors were similar to those presented in this work, it says, amorphous phase obtaining until 1–1.5 mm thickness. There were no detectable crystalline diffraction peaks and diffuse signals were observed around 38° and 66°; while in the present study diffuse signals were observed around 38° and 70°.

The microstructure observed in the thicker region of the wedge shows a crystalline structure, as detected in XRD analysis (Fig. 4). The light regions of the eutectic composition, observed in Fig. 5c, are probably composed of MgZn, while the dark regions are composed of pure Mg. The $Mg_6Zn_3Ca_2$ phase is not easily seen because of instrumental resolution.

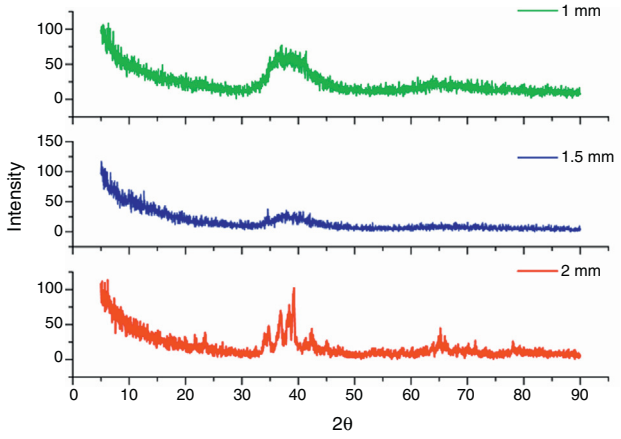

Fig. 4 – Diagram of X-ray diffraction corresponding to three different regions of the wedge showing the presence of amorphous phase for 1 and 1.5 mm thickness and crystalline phases beyond the latter.

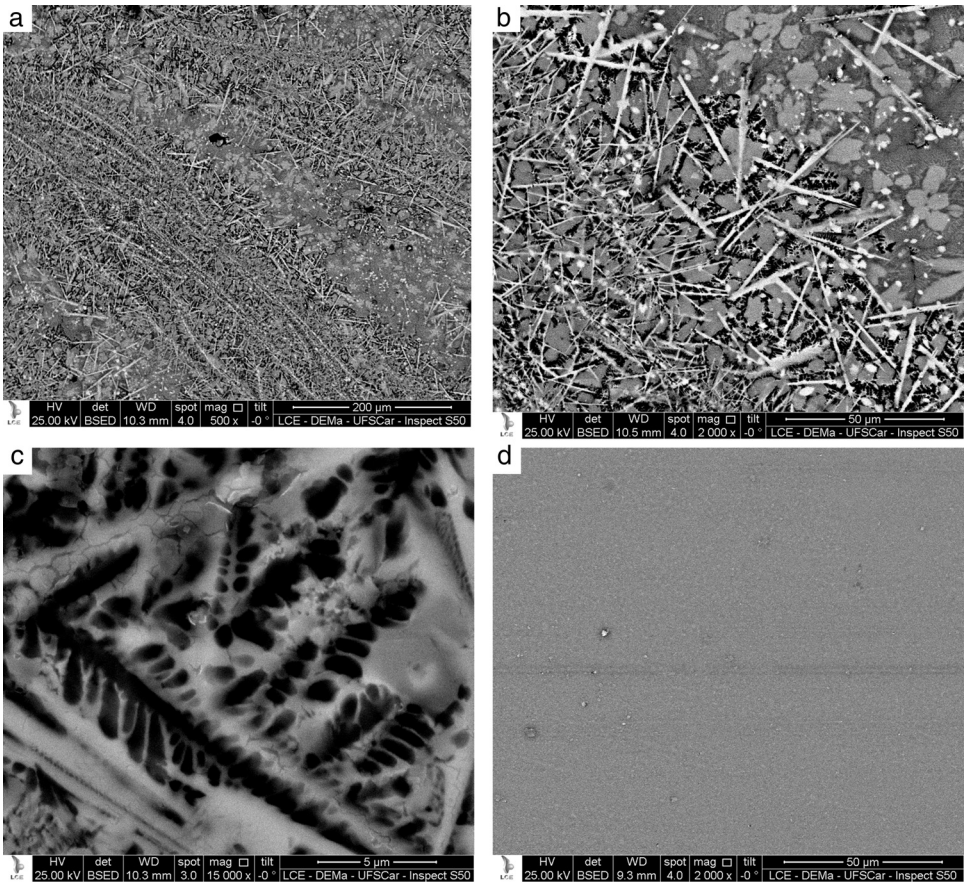

Fig. 5 – SEM images (BSED) of the crystalline sample (a) 500×, (b) 2000×, (c) 15,000×, and (d) 10,000× (amorphous).

In Fig. 5b, it is possible to observe the primary MgZn phase with a needle-like geometry. The amorphous microstructure observed in Fig. 5d corroborates the XRD results of the melt-spun ribbon showed in Fig. 2 and XRD results of the three different regions of the wedge showed in Fig. 4.

DSC analyses were conducted in different regions of the wedge (Fig. 6) and the results show the presence of glass transition until 1.5 mm, which indicates the presence of amorphous phase. It can be seen that T_g and T_x of the BMG were 146 °C and 162 °C, respectively, resulting in a thermoplastic forming (TPF) window (or supercooled liquid region) of ~16 °C, close to those found by Cao et al. [16] (~15 °C) and Qin et al. [15] (~17 °C). This TPF window is not as wide compared with other Mg alloys containing elements such as Cu and rare earth (RE); for example, $Mg_{65}Cu_{25}Gd_{10}$ developed in some experimental conditions by Xi et al. [14] showed TPF window between 74 and 82 °C. However, these elements are not suitable for biomedical implants due to lack of biocompatibility. The results obtained indicated that the melting range of the material processed lies between 342 and 391 °C, with an exothermic peak at 351 °C.

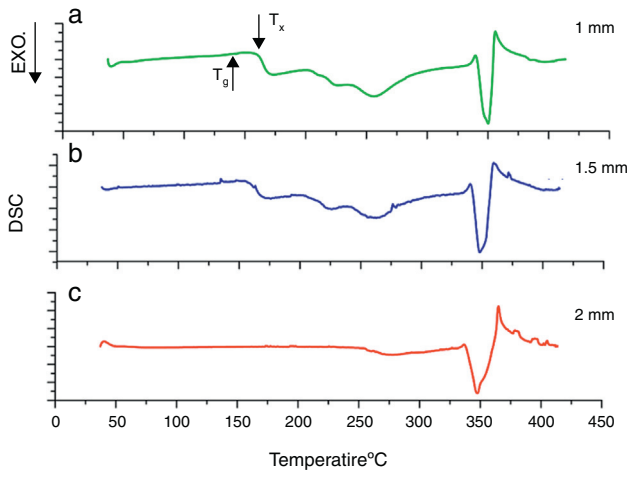

Fig. 6 – DSC thermograms of the different thicknesses of the wedge cast sample.

Cao et al. [16] produced amorphous $Mg_{65}Zn_{30}Ca_5$ discs of 1 mm thickness, while Qin et al. [15] processed cylindrical samples of 2 mm in diameter and observed the presence of amorphous phase. These results agree with those obtained in this work. Further attempts were carried out after we mastered well the fusion process and wedge like samples with amorphous structure until 2.5 mm were obtained, as shown in Fig. 7.

The class of Mg–Zn–Ca alloys is one of several systems, characterized by a high GFA with the biocompatible composition. However, bulk metallic glasses based on the Mg–Zn–Ca system are a relatively new class of amorphous alloys, which are characterized by very high strength properties, high

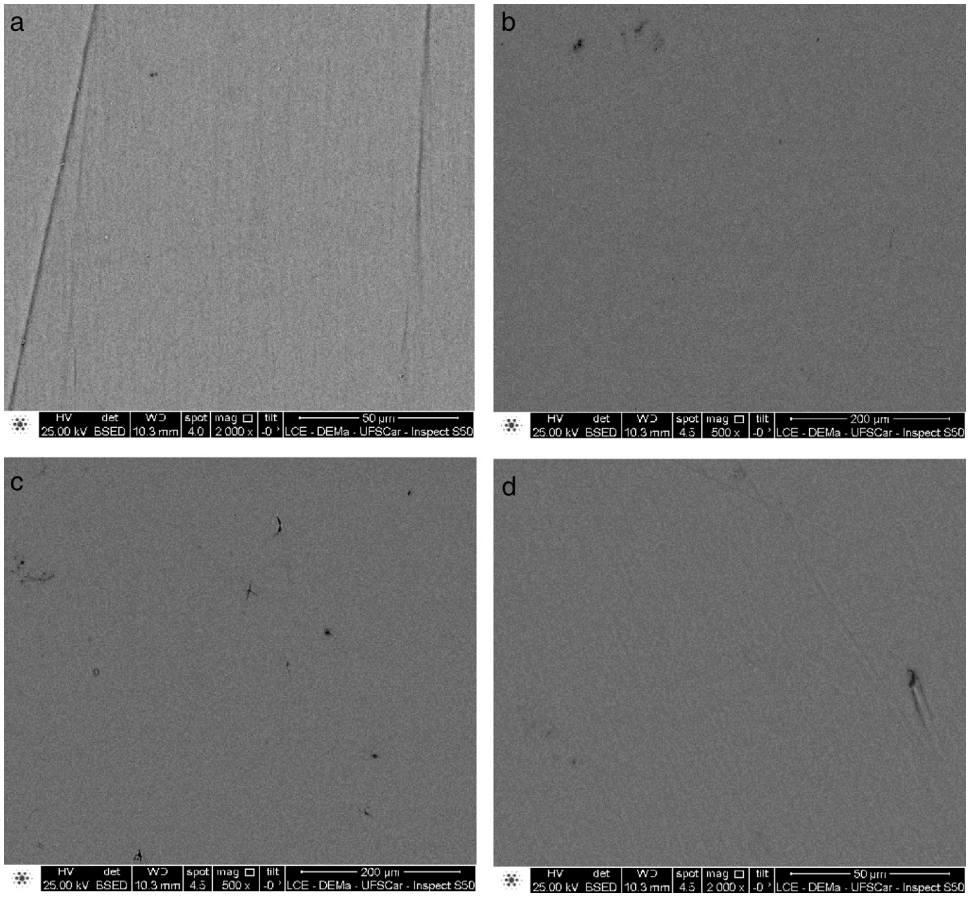

Fig. 7 – SEM images (BSED) of the amorphous phase observed at different regions of the wedge: (a) 1.8 mm, (b) 2.0 mm, (c) 2.5 mm (500×), (d) 2.5 mm (2000×).

toughness and high glass forming ability. Therefore, establishing the most appropriate procedure for obtaining amorphous material as well as electing the most efficient techniques for its characterization is of fundamental importance for the study of a new material for bioabsorbable implant application.

4. Conclusion

Based on the results previously presented, we can conclude that the system adopted for obtaining the alloy of interest ($Mg_{65}Zn_{30}Ca_5$), starting from the preparation of binary alloys, was efficient in view of the experimental values for the alloy elements, which were consistent with the target values. This procedure allowed working at low temperatures, reducing losses and oxidation, which can hinder the achievement of the amorphous phase. The use of SF_6 added to argon, which is commonly used in this type of melting, showed no significant improvement in the oxygen content of processed alloys. Oxygen contents of 10 and 25 ppm were obtained for alloys processed under argon + SF_6 and Argon atmosphere, respectively. The results of DSC, XRD and SEM showed the presence of amorphous phase up to 1.5 mm thickness, with amorphous structures observed up to 2.5 mm when the melting process was better mastered.

Funding

CNPq – Conselho Nacional de Desenvolvimento Científico e Tecnológico – Ñational Counsel of Technological and Scientific Development:

Capes – Coordenação de Aperfeiçoamento de Pessoal de Nível Superior.

Conflicts of interest

The authors declare no conflicts of interest.

Acknowledgments

The authors are grateful to CNPq (Universal Project) for the financial support and Capes for the scholarship granted to TBM.

REFERENCES

[1] Staiger MP, Pietak AM, Huadmai J, Dias G. Magnesium and its alloys as orthopedic biomaterials: a review. Biomaterials 2006;27:1728–34.

[2] Peng Q, Huang Y, Zhou L, Hort N, Kainer KU. Preparation and properties of high purity Mg–Y biomaterials. Biomaterials 2010;31:398–403.
[3] Zhang L-N, Hou Z-T, Ye X, Xu Z-B, Bai X-L, Shang P. The effect of selected alloying element additions on properties of Mg-based alloy as bioimplants: a literature review. Front Mater Sci 2013;7:227–36.
[4] Li Z, Gu X, Lou S, Zheng Y. The development of binary Mg–Ca alloys for use as biodegradable materials within bone. Biomaterials 2008;29:1329–44.
[5] Song G. Control of biodegradation of biocompatable magnesium alloys. Corros Sci 2007;49:1696–701.
[6] Zberg B, Uggowitzer PJ, Löffler JF. MgZnCa glasses without clinically observable hydrogen evolution for biodegradable implants. Nat Mater 2009;8:887–91.
[7] Basu J, Ranganathan S. Bulk metallic glasses: a new class of engineering materials. Sâdhanã 2003;28:783–98.
[8] Waizy H, Seitz JM, Reifenrath J, Weizbauer A, Bach FW, Meyer-Lindenberg A, et al. Biodegradable magnesium implants for orthopedic applications. J Mater Sci 2012;48:39–50.
[9] Danez GP [M.Sc. dissertation] Tendência de Formação de Fase Amorfa em Ligas a Base de Magnésio para Biomaterial Temporário. São Carlos, SP, Brasil: DEMa/UFSCar; 2011.
[10] Gu X, Zheng Y, Zhong S, Xi T, Wang J, Wang W. Corrosion of, and cellular responses to Mg–Zn–Ca bulk metallic glasses. Biomaterials 2010;31:1093–103.
[11] Yang L, Huang Y, Peng Q, Feyerabend F, Kainer KU, Willumeit R, et al. Mechanical and corrosion properties of binary Mg–Dy alloys for medical applications. Mater Sci Eng B 2011;176:1827–34.
[12] Sun Y, Zhang B, Wang Y, Geng L, Jiao X. Preparation and characterization of a new biomedical Mg–Zn–Ca alloy. Mater Des 2012;34:58–64.
[13] Fang D, Li X, Li H, Peng Q. Electrochemical corrosion behavior of backward extruded Mg–Zn–Ca alloys in different media. Int J Electrochem Sci 2013;8:2551–65.
[14] Xi XK, Wang RJ, Zhao DQ, Pan MX, Wang WH. Glass-forming Mg–Cu–RE (RE = Gd, Pr, Nd, Tb, Y, and Dy) alloys with strong oxygen resistance in manufacturability. J Non-Cryst Solids 2004;344:105–9.
[15] Qin F, Xie G, Dan Z, Zhu S, Seki I. Corrosion behavior and mechanical properties of Mg–Zn–Ca amorphous alloys. Intermetallics 2013;42:9–13.
[16] Cao JD, Martens P, Laws KJ, Boughton P, Ferry M. Quantitative in vitro assessment of $Mg_{65}Zn_{30}Ca_5$ degradation and its effect on cell viability. J Biomed Mater Res B: Appl Biomater 2013;101:43–9.